Thermal simulations for characterization of ATHENA mirror modules with a radiating box in the BEaTriX facility

S. Basso, B. Salmaso

S. Basso, B. Salmaso, "Thermal simulations for characterization of ATHENA mirror modules with a radiating box in the BEaTriX facility," Proc. SPIE 11119, Optics for EUV, X-Ray, and Gamma-Ray Astronomy IX, 111191I (9 September 2019); doi: 10.1117/12.2530622

SPIE.

Event: SPIE Optical Engineering + Applications, 2019, San Diego, California, United States

Thermal simulations for characterization of ATHENA Mirror Modules with a radiating box in the BEaTriX facility

S. Basso[a], B. Salmaso[a],
[a]INAF/Brera Astronomical Observatory, Via E. Bianchi 46, 23807 Merate, Italy

ABSTRACT

The BEaTriX facility is currently in the realization phase at INAF – Osservatorio Astronomico di Brera in Merate (Italy) and it will be used as demonstrator for the acceptance test (PSF and Aeff) of the ATHENA Mirror Modules (MMs), with a rate of 3 MMs/day. The BEaTriX facility is a compact X-ray test facility (13m x 6 m x 2m) working in low vacuum at the energies of 1.5 keV and 4.5 keV. The testing optic is placed into a small chamber (MM chamber), that allows a fast MMs replacing time. All the MMs will be tested at room temperature (20°C), but the possibility of X-ray characterization at different temperature (-10°C / +50°C) is also foreseen. For this task a modular thermal box is designed and will be installed inside the MM chamber. The thermal box radiatively heats or cools the MM, by means of heat pipes that transfer the desired heat from dedicated chillers. It is designed to be able to impose a uniform temperature across the MM or impose also some gradient in order to characterize the optical performance of the MM in different thermal condition. In this paper, we present simulations of the temperature distribution at the MM level, as function of the thermal box design, which has been optimized considering the space envelope and result of the FEM simulations.

Keywords: Athena, Beatrix, x-ray optic, Mirror module, SPO, thermal simulation, FEM

1. INTRODUCTION

The Mirror Modules of the ATHENA (Advanced Telescope for High-ENergy Astrophysics) are made with Silicon Pore Optic (SPO) technology, developed by ESA in these years in order to reach the demanding optical resolution of the Athena X-ray telescope[1][2]. In order to characterize the MM quality, the demonstrating facility BEaTriX (Beam Expander Testing X-ray facility) has been designed to provide a wide parallel X-ray beam (at 4.51 keV and 1.49 keV) with a pupil size large enough to cover the overall print-through of the ATHENA MMs. BEaTriX is currently in the construction phase and will be installed in the INAF-OAB laboratory[3][4][5]. The size of the pupil is 170 mm x 60 mm while the MMs pupil size goes from 48.9 x 54 mm (MM#1) to a maximum of 116.4 x 54 mm (MM#15).
The overall Half Energy Width (HEW) of the ATHENA X-ray telescope is 5 arcsec and the requested performance of the facility is to provide a beam divergence less than 1.5 arcsec (HEW). The MM under test is mounted with a dedicated interface onto a hexapod able to provide the needed alignment. The possibility to test the MMs at different temperature is a required capability useful to understand the effect of temperature variation on the image PSF. To perform this task a thermal box has been designed with the possibility to maintain the MM at a temperature ranging from -10 °C to 50 °C, by means of heat radiation. The facility works in a vacuum level of 10^{-3} mbar, there is no convection and the heat conduction is kept very low by a proper design of the interfaces. Minimizing the conducting flux is essential to reduce spurious thermal gradients. The thermal box is heated/cooled by means of liquid lines, connected to an external thermostat and passing through the edge of the box. Even if the BEaTriX is designed to test 3 MMs per day, the thermal tests will be performed only for some samples. In this framework the speed for the thermalization at -10 °C or +50 °C is not an issue and it has been considered acceptable if the needed time is maintained within one day. Nevertheless, the necessity to mount the MM under test and handle it, when the thermal box is installed, is a driver constraint, considering also the small size of the MM chamber (Φ750mm x 650mm height). The position of the thermal box inside BEaTriX is shown in Figure 1. The implementation of the thermal box inside BEaTriX is foreseen for the end of 2020, after the test phase.

Optics for EUV, X-Ray, and Gamma-Ray Astronomy IX, edited by Stephen L. O'Dell, Giovanni Pareschi, Proc. of SPIE
Vol. 11119, 111191I · © 2019 SPIE · CCC code: 0277-786X/19/$21 · doi: 10.1117/12.2530622

2. MECHANICAL DESIGN

The thermal box surrounds the MM under test, which is connected through a dedicated interface to a hexapod positioned onto an optical bench, decoupled from the MM Chamber.
A modular approach has been followed in order to give to the system enough flexibility for future changes. Only one liquid line is foreseen as baseline, but it is easy to implement different liquid lines (up to 8) switching in the four main nodes the tubes connection from one end of the tubes to the other (Figure 2). For this purpose 8 feedthrough are available on the chamber's wall. The green panels in Figure 2 are removable plates, with the scope of give access to the MM and also to eventually impose some gradient in left/right or up/down directions. Additional heaters can be used to increase the thermal gradient.

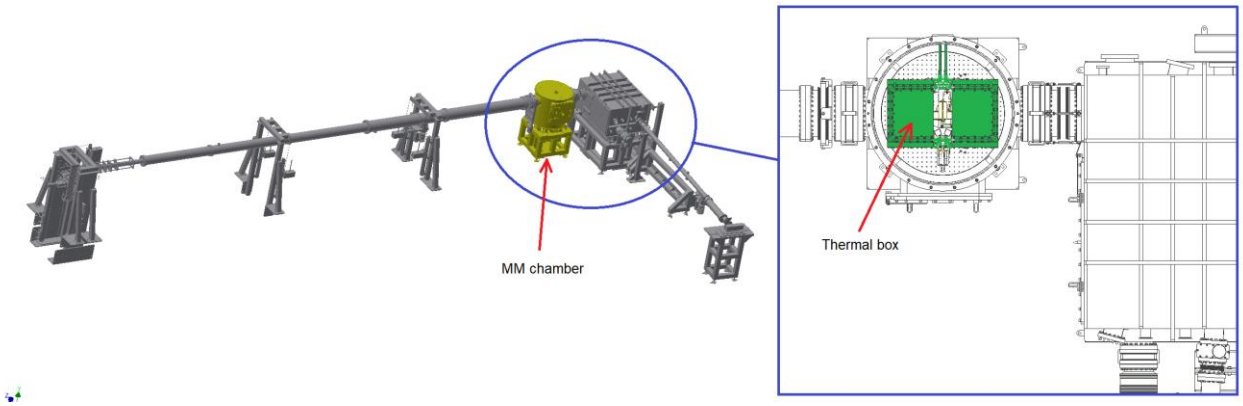

Figure 1 – BeaTriX facility and position of the thermal box

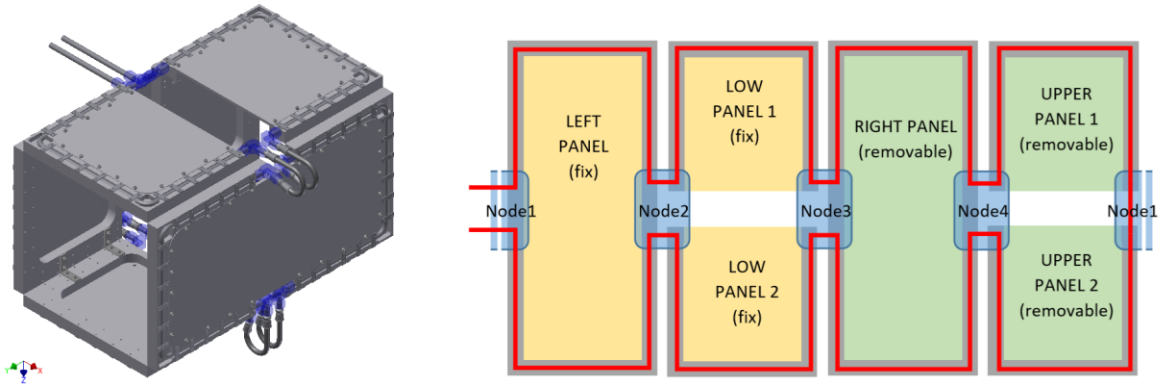

Figure 2 – Mechanical design of the thermal box and scheme of the liquid line.

The used material is Aluminum for its high thermal conductivity and low mass. The total weight of the thermal box is 26 kg and it can be sustained by an independent structure directly fixed on the inner side of the chamber wall: in this way it is totally decoupled from the optical bench on which the MM and its motorization are mounted. The motorization is kept outside the thermal box in order to maintain its temperature near the 20°C and to improve the efficiency of the thermal box avoiding internal heat sources. The interface parts connecting the motorization and the MM pass through the bottom aperture in the low panel of the thermal box (Figure 3). In the upper panel a same aperture is foreseen to preserve symmetry.
The size of the thermal box is 365 x 365 x 600 mm. The internal surfaces are treated with black anodization, or low outgassing paints, in order to increase the emissivity. While low outgassing paints provide a better performance in term of emissivity and outgassing, the low level of vacuum and the possibility to scratch due to mounting and-dismounting make the anodization the baseline solution.

The chiller must be capable to reach temperatures of about -50°C, necessary to cool the MM down to – 10 °C only by radiation. The selected chiller is an open bath system and it is visible in Figure 4 with the list of some possible liquids. While heating is well in specification with this chiller, it is near the theoretical limit for reaching the lower temperature. The interface parts are made in Titanium, with insulating washers as connections, in order to reduce the conductive flux through the interface. This decoupling is important because the power dissipated by the selected Hexapod is 6W at the rest, and the heat flux must mainly go through the base to the optical bench instead of going to the MM. The overall conductance of the interface parts from the MM to the motorization is shown in Figure 5.

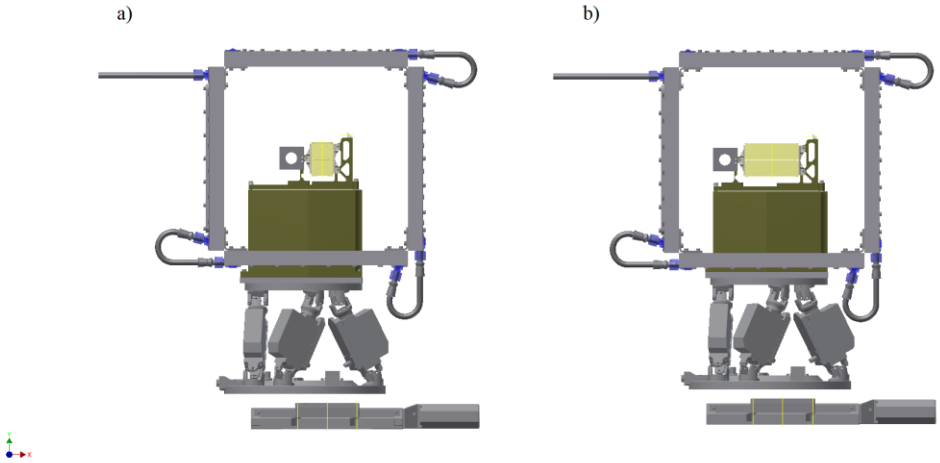

Figure 3 – Front view of the thermal box with MM#1 (a) or MM#15 (b) mounted. The interface parts (green) pass through an aperture in the lower panel.

name	LAUDA RP245E
Temperature range min/max [°C]	-45/200
Stability [°C]	0.05
Heating power [kW]	2.5
Cooling power @20°C [kW]	0.8
Max pump flow [l/min]	22
Max pump pressure [bar]	0.7/0.4
Volume min/max [l]	2.4/4.4
Size [mm]	300x430x675
Weight [kg]	46
Elecric Power [kW]	3.7
Power supply	230 V - 50 Hz

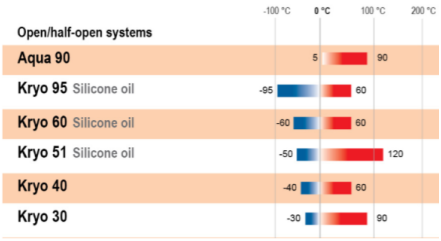

Figure 4 – Chiller for cooling/heating with possible liquids

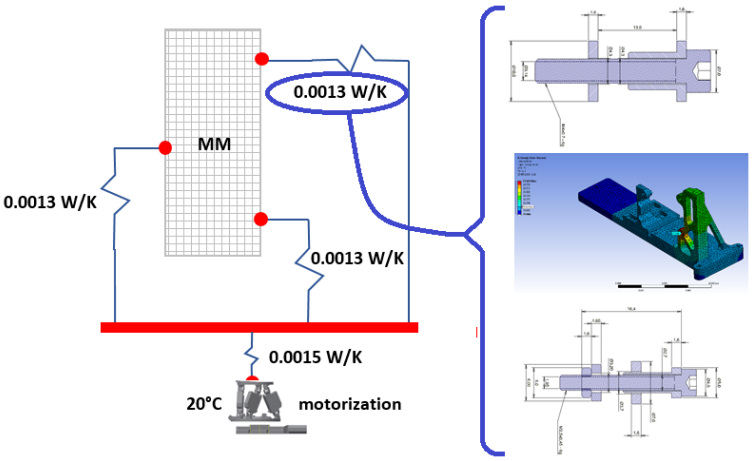

Figure 5 – equivalent conductance of interface parts

3. FEM DESCRIPTION

ANSYS 17.2 is used for Finite Element Analysis. The model is simple, in order to keep computing time low with a number of nodes/elements of 7956/9208. The extremely low number of nodes is obtained simplifying the MM with an equivalent solid without the modelization of all the Silicon layers and ribs (Figure 6). In order to take into account the pore geometry, the emissivity is not the same for all the direction: the surfaces corresponding to the front/rear pores has a different emissivity w.r.t. the other Silicon surfaces.

a) b)

Figure 6 –MM simplified model. Each Si stack is composed by thousands of pores (a). The Finite Element Model is composed by much less solid elements (b). The emissivity of the pores side is different from the other Silicon surfaces.

To simplify the pores with solid elements, also the thermal conductivity is considered anisotropic with different values in radial (Y), axial (Z) or azimuthal (X) direction. The equivalent thermal conductivity has been computed using the geometry shown in Figure 7.

s1 [mm]	s2 [mm]	t1 [mm]	t2 [mm]
0.17	0.605	0.17	1

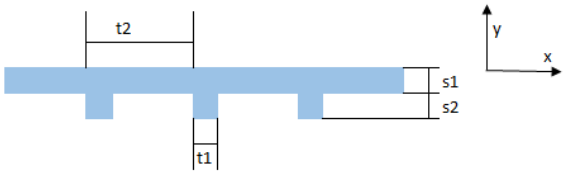

Figure 7 – geometry of pores used for equivalent thermal conductivity computation.

The pure Silicon conductivity is 124 W/mK. Considering the geometry it becomes 31.4, 25.8 and 43.7 W/mK for X, Y and Z direction, respectively. Figure 8 shows the mesh for the two considered MMs.

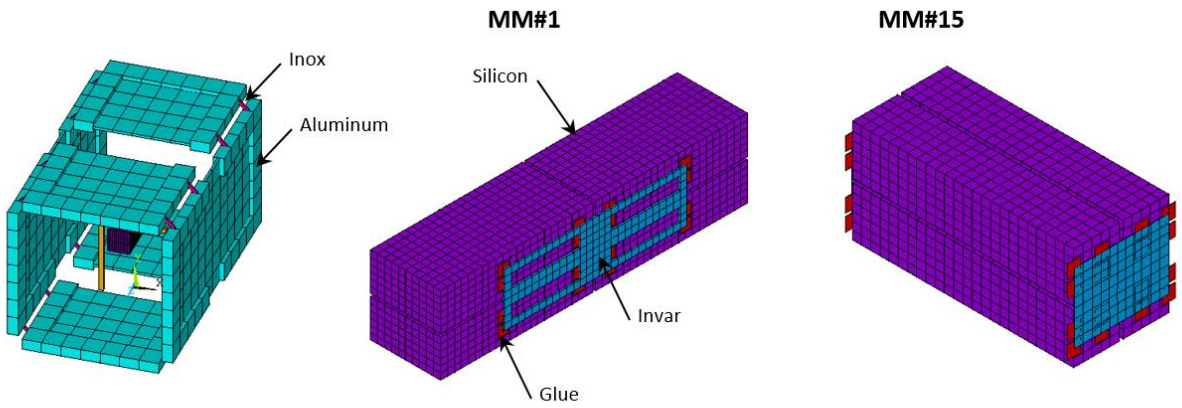

a) b) c)

Figure 8 – Mesh for the thermal model: thermal box (a), MM#1 (b) and MM#15 (c). Different materials are shown with different colors

4. RESULTS

Acceptance tests for all the ATHENA MMs will be performed, in BEaTriX, at the nominal operative temperature. Only some MMs will be tested under different thermal conditions, which means (see Section 1) at different temperature and with some thermal gradient. The goal for the thermal gradient is 10 K/m. In this section, the results of the simulations are presented considering different MMs, different load conditions and removing the panels in order to increase the thermal gradients. An estimate of the needed time is presented.

4.1 THERMAL CYCLE TIME

Considering the pipe line and imposing a temperature in the corresponding nodes on the box, the simulations show the dependence of the MM temperature on the thermal box temperature (Figure 9a) for a steady state condition. The cooling/heating power of the chiller depends on the temperature, and a transient condition (Figure 9b) must be taken into account considering also the great mass of the thermal box. The real behaviour during the heating or cooling cycle is in between the case with constant temperature and constant heat power.

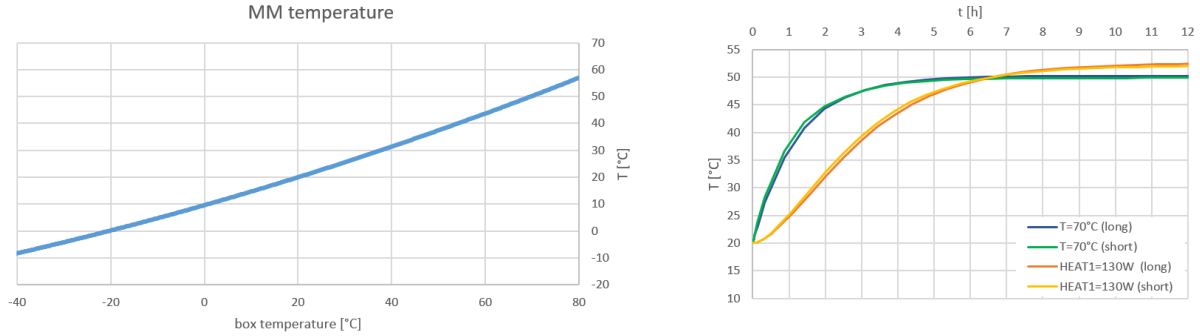

a) b)

Figure 9 – relationship between box temperature and MM temperature with no other heat source (a) and heating time for the MM#1 (long) and MM#15 (short) in the case of fix temperature of the pipe line (70°C) or constant heat power (130W) (b)

In order to better understand the transient, a simulation with chiller power as function of the temperature has been run for different type of chillers (Figure 10). The heating/cooling time can be estimated in 4/6 hours.

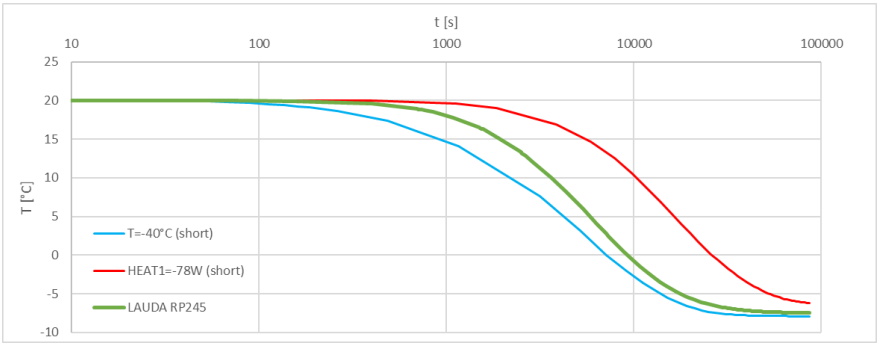

Figure 10 – MM temperature during cooling cycle for the case of LAUDA RP245 chiller compared to the case of fix temperature of the pipe line (-40°C) or constant heat power (-78W)

4.2 HOT AND COLD CASE

For the nominal case of constant heating, the distribution of temperature in the MMs is shown in Figure 11. Considering that the model is almost symmetric, the temperature distribution in the Silicon stack is expected to be symmetric. A rough estimate of the Half Energy Width (HEW) can be computed from the median of the thermal gradient (∂T_z) along the axial direction, with the hypothesis that the changes in longitudinal slopes mostly affect the HEW. Considering the coefficient of thermal expansion (α) of the Silicon ($3 \cdot 10^{-6}$), the slope change (ϑ) for each element is

$$\vartheta \simeq \partial T_z \cdot \alpha \tag{1}$$

We also assume that the effect of the 4 stacks (XOU), 2 on the parabolic side and 2 on the hyperbolic side, are independent, and therefore compute the HEW for each stack as:

$$HEW_i = 4 \cdot median(|\vartheta|), \qquad i = 1, \ldots, 4 \tag{2}$$

The HEW estimate of the MM is computed by the root square sum of the four stacks. It must be noted that only thermal contributions on Silicon are accounted in this formalism, while thermo-elastic effects due to the supports are not considered.

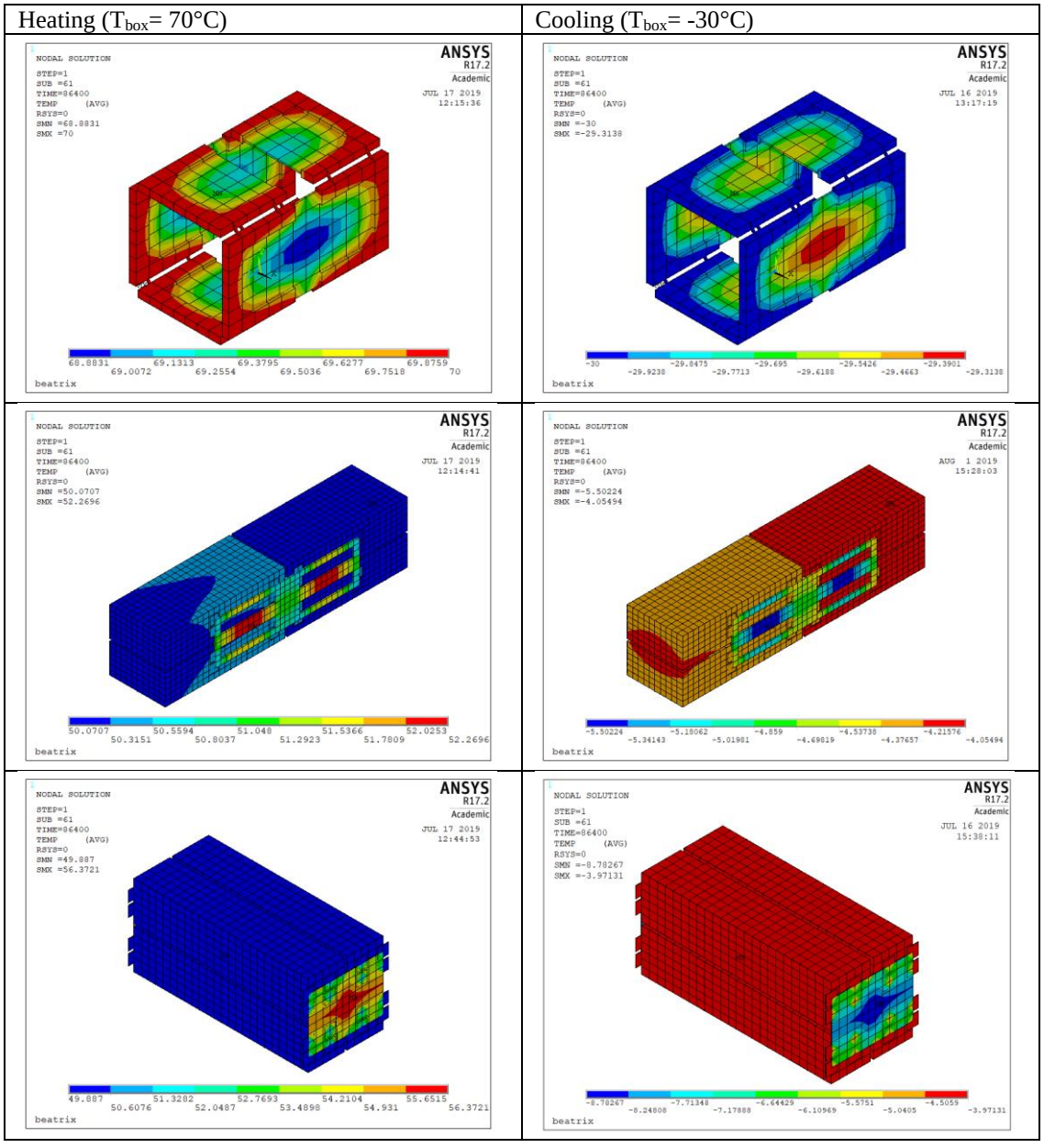

Figure 11 – Temperature distribution for uniform heating/cooling

Table 1 – Thermal gradient occurring on the MMs, during uniform heating/cooling of the MMs with the thermal box. The thermal gradient is computed as the median on the elements, taken with their absolute values.

	Heating (MM at 50 °C)		Cooling (MM at -10 °C)	
	MM#1	MM#15	MM#1	MM#15
thermal gradient [K/m]	2.2	2.0	1.5	1.4
thermal gradient (Z) [K/m]	0.53	0.28	0.39	0.18
HEW [arcsec]	2.6	1.4	1.9	0.9

4.3 INCREASING THERMAL GRADIENT

Other simulations have been run to understand the possibility to increase the thermal gradient removing one of the two removable panels. This is possible in the hot or cold case, because the side without the panel sees directly the surrounding chamber considered at a temperature of 20°C. Figure 12 shows the temperature distribution on the box itself, during heating cycle.

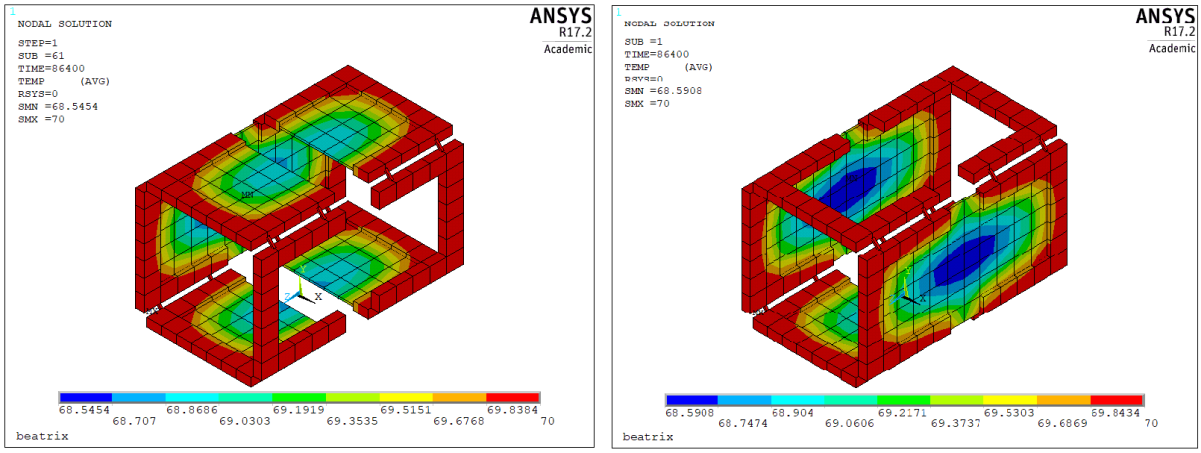

a) b)

Figure 12 – Temperature on the thermal box in the hot case when lateral panel (a) or upper panel (b) are removed

The effect of removing the top panel is much more efficient because in the vertical (Y) direction there are two XOUs separated without any conductive link, the heat flux passes through the glue and the Invar structure by conduction. When the lateral panel is removed the heat flux passes through the Silicon itself, which has a high conductivity, producing in the MM a much lower gradient in the horizontal direction (Figure 13a) w.r.t. vertical direction where a step in the temperature is visible (Figure 13b).

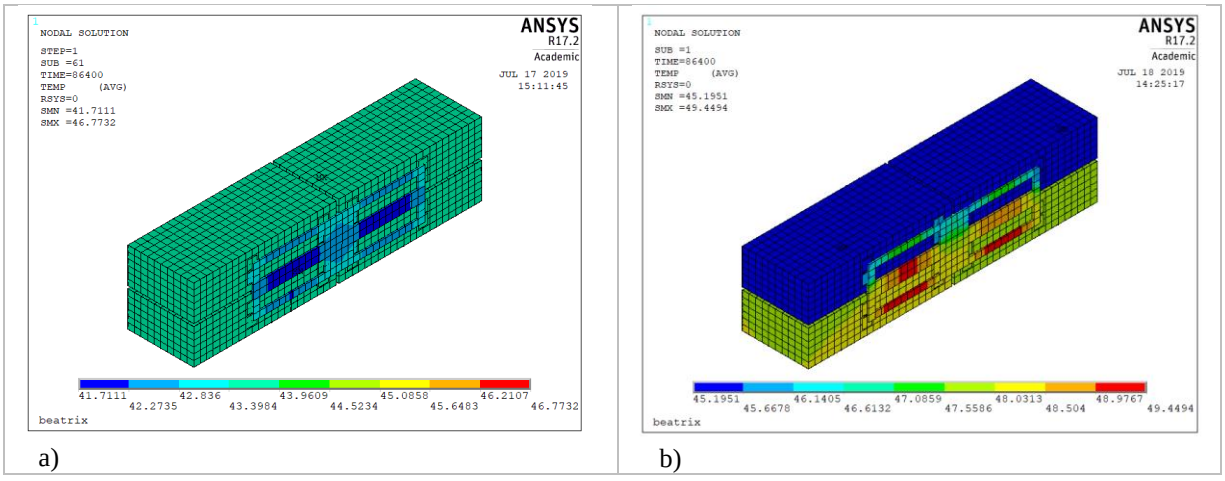

a) b)

Figure 13 – Temperature distribution in the MM#1 for the case of lateral panel removed (a) and top panel removed (b)

Summarizing the effect of removing panel, the significant parameter (δT) is considered as the temperature difference in Silicon divided by significant length (l_k, height when top panel is removed or width when lateral panel is removed). The significant parameter (δT) is therefore (see Figure 14):

$$\delta T = \frac{T_{MAX\_Si} - T_{MIN\_Si}}{l_k} \quad (3)$$

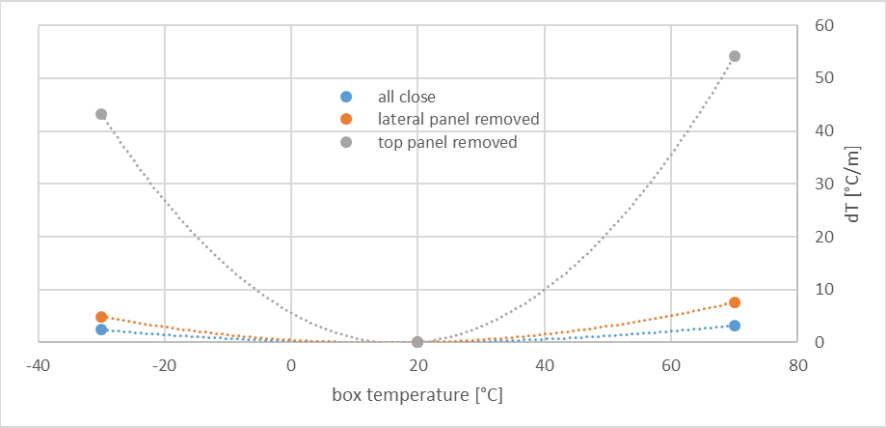

Figure 14 – increase of temperature difference in Silicon (δT) when lateral panel or top panels are removed

5. CONCLUSION

The realization of the first beam line, at 4.51 keV, of the BEaTriX facility is ongoing at INAF-OAB. The optical thermal characterization of some MMs at thermal conditions different from nominal, is addressed with a dedicated thermal box, able to impose a temperature range of 60°C to the MMs. The thermal box is decoupled from the MM and its supporting structure, in order to avoid interferences. The possibility to remove two panels provides the benefit to increase the thermal gradient without introducing other regulating system, like multi-chiller or heaters. The modular approach of the thermal box design enable future upgrades in order to further increase the thermal gradients. The box can be possibly used also to compensate heat source from the MM motorizations.

ACKNOWLEDGMENT

The development of the BEaTriX facility is funded by the ESA contract No. 4000123152/18/NL/BW, “Advanced and Compact X-ray Test facility for the ATHENA SPO module”.

REFERENCES

[1] Bavdaz, M., Wille, E., Ayre, M., Ferreira, I., Shortt, B., et al., “Development of the ATHENA mirror”, Proc. SPIE 10699, 106990X (2018)
[2] Collon, M., Vacanti, G., Barriere, N., Landgraf, B., Guenther, R., et al., “Silicon pore optics mirror module production and testing”, Proc. SPIE 10699, 106990Y (2018)
[3] Spiga, D., Pelliciari, C., Salmaso, B., et al. “Design and advancement status of the Beam Expander Testing Xray facility (BEaTriX)”, Proc. SPIE 9963, 996304 (2016)
[4] Salmaso, B., Spiga, D., Basso. S., Ghigo, M., Giro, E., Pareschi, G., Tagliaferri, G., Vecchi, et al., “BEaTriX (Beam Expander Testing X-ray facility) for testing ATHENA’s SPO modules: advancement status”, Proc. ICSO, (2018)
[5] Salmaso, B., Basso, S., Giro, E., Spiga, D., Sironi, G., Vecchi, G., Ghigo, M., Pareschi, G., Tagliaferri, G., Uslenghi, M., Fiorini, M., Paoletti, et al. “BEaTriX, the Beam Expander Testing X-ray facility for testing ATHENA’s SPO modules: progress in the realization”, Proc. SPIE, this conference (2019).